Journal of proteome research

pubs.acs.org/jpr

Article

Phosphoproteomic Analysis Defines BABAM1 as mTORC2 Downstream Effector Promoting DNA Damage Response in Glioblastoma Cells

Nuttiya Kalpongnukul, Rungnapa Bootsri, Piriya Wongkongkathep, Pornchai Kaewsapsak, Chaiyaboot Ariyachet, Trairak Pisitkun, and Naphat Chantaravisoot*

Cite This: *J. Proteome Res.* 2022, 21, 2893−2904

Read Online

ACCESS | Metrics & More | Article Recommendations | Supporting Information

ABSTRACT: Glioblastoma (GBM) is a devastating primary brain cancer with a poor prognosis. GBM is associated with an abnormal mechanistic target of rapamycin (mTOR) signaling pathway, consisting of two distinct kinase complexes: mTORC1 and mTORC2. The complexes play critical roles in cell proliferation, survival, migration, metabolism, and DNA damage response. This study investigated the aberrant mTORC2 signaling pathway in GBM cells by performing quantitative phosphoproteomic analysis of U87MG cells under different drug treatment conditions. Interestingly, a functional analysis of phosphoproteome revealed that mTORC2 inhibition might be involved in double-strand break (DSB) repair. We further characterized the relationship between mTORC2 and BRISC and BRCA1-A complex member 1 (BABAM1). We demonstrated that pBABAM1 at Ser29 is regulated by mTORC2 to initiate DNA damage response, contributing to DNA repair and cancer cell survival. Accordingly, the inactivation of mTORC2 significantly ablated pBABAM1 (Ser29), reduced DNA repair activities in the nucleus, and promoted apoptosis of the cancer cells. Furthermore, we also recognized that histone H2AX phosphorylation at Ser139 (γH2AX) could be controlled by mTORC2 to repair the DNA. These results provided a better understanding of the mTORC2 function in oncogenic DNA damage response and might lead to specific mTORC2 treatments for brain cancer patients in the future.

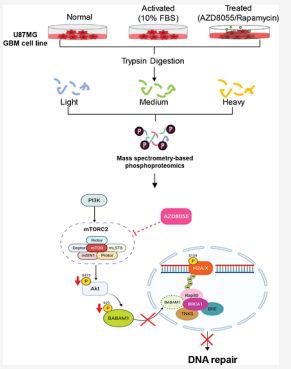

KEYWORDS: *phosphoproteomics, glioblastoma, DNA damage response, mTORC2, BABAM1*

INTRODUCTION

Glioblastoma multiforme (GBM) is a primary brain tumor originating from astrocytes. GBM is classified into high-grade IV gliomas. They are malignant tumors and an aggressive form of brain tumors with a high proliferation rate. GBM patients usually have a short life expectancy after diagnosis. More than two-thirds of adults diagnosed with glioblastoma die within 2 years because they grow rapidly and spread to other parts of the brain.[1] Due to the invasive nature of the tumor, it has a high recurrence rate and a poor prognosis. To date, there is no specific cure for GBM.

The mechanistic target of rapamycin (mTOR) kinase is the major mediator of phosphatidylinositol 3-kinase (PI3K) signaling pathway.[2] The mTOR pathway is one of the most frequently altered signaling cascades in humans. It integrates both intracellular and extracellular signals and serves as a central regulator of cell metabolism, growth, proliferation, and survival. The main component of the pathway, mTOR protein kinase, forms the core of two distinct multiprotein complexes, mTOR complex 1 (mTORC1), and mTOR complex 2 (mTORC2).[3,4]

The regulation and roles of mTORC1, its many upstream regulators, cellular functions, and the availability of rapamycin as an inhibitor are well known, and this complex has been thoroughly investigated. On the other hand, mTORC2 has been proposed to play an essential role in carcinogenesis, tumor growth promotion, and chemotherapy resistance in glioblastoma cells.[4] Multiple studies have indicated that mTORC2 is a potential target for molecular therapeutics in GBM. The mTOR inhibitor PP242 effectively targets both mTORC1 and mTORC2 activation and reduces cell proliferation, migration, invasiveness, and stemness properties in GBM.[5] Also, mTORC2 drives GBM growth by promoting histone acetylation and nuclear translocation.[6] More recently, mTORC2 has been shown to play a new role in DNA damage response (DDR) and repair. Inhibitors of DNA damage response (DDR) have a high potential for radiosensitization of various cancers, including glioblastoma (GBM).[7]

Several studies have identified the phosphopeptidome and localized the phosphorylation sites associated with cancer cells using mass spectrometry-based phosphoproteomics. Also,

Received: April 24, 2022
Published: October 31, 2022

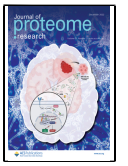

quantitative phosphoproteome profiling allows researchers to study abnormally activated signaling pathways, discover therapeutic targets in cancer, and identify the regulators of essential signaling pathways and cellular processes.[8,9] Although various phosphoproteomics studies have been performed so far, there are no complete insights into the phosphorylation-related mTORC2 signaling with biological functions in GBM. Global phosphoproteomics study fills a gap in our understanding of this mTOR complex and may be relevant to mTORC2 activities in other diseases.

In this study, we performed quantitative phosphoproteomic analyses of glioblastoma cells under different conditions related to mTORC2 activation status using a high-resolution nanoflow LC−MS/MS system combined with a labeling technique and phosphopeptide enrichment. We also determined several affected biological processes in response to mTORC2 inhibition. Consequently, we were able to identify the proteins with altered phosphorylation patterns involved in DNA damage response (DDR) through mTORC2-mediated mechanisms in GBM and pursued the investigation focusing on BABAM1 (also known as MERIT40) and H2AX phosphorylation. The ultimate goal of this study is to reveal potential downstream targets of mTORC2 responsible for promoting DNA damage control and repair that may confer more aggressive properties to GBM.

MATERIALS AND METHODS

Cell Culture

U87MG (HTB-14), a glioblastoma multiforme (GBM) cell line, was obtained from ATCC. U87MG cells were maintained in DMEM low glucose, supplemented with 10% fetal bovine serum (FBS), and 1% antibiotic−antimycotic. For activation and treatment experiments, cells were starved in DMEM without 10% FBS for 24 h. For activation condition, cells were starved in serum-free DMEM for 24 h, followed by replacing the media with regular media (DMEM low glucose containing 10% FBS) for 1, 6, or 24 h. For the mTORC1/2 inhibition condition, cells were starved for 24 h and then cultured in DMEM low glucose, supplemented with 10% FBS and 2 μM AZD8055 for 1, 6, or 24 h. For the mTORC1-inhibiting condition, cells were starved for 24 h, then grown in DMEM, and supplemented with 10% FBS and 0.1 μM rapamycin for 1, 6, or 24 h.

Quantitative Phosphoproteome Sample Preparation

The U87MG cells were lysed with 8 M urea, 100 mM TEAB, 1× protease inhibitor, and 1× phosphatase inhibitor. Lysates were centrifuged at 13,000g for 5 min at 4 °C. Protein concentrations were determined by the bicinchoninic acid (BCA) protein assay kit (Pierce). Protein samples were adjusted to 1 mg in 8 M urea lysis buffer per condition. The proteins were reduced with 10 mM dithiothreitol, alkylated with 40 mM iodoacetamide, and digested with sequencing-grade modified trypsin (Promega) overnight. Tryptic peptides were subsequently cleaned up with reversed-phase C18 SPE columns. Peptide concentrations were determined by Quantitative Fluorometric Peptide Assay (Pierce). Finally, peptides were dried using Speed-Vac for long-term storage at −20 °C. Digested samples were reconstituted with 100 μL of 100 mM TEAB. For isotope labeling, peptides were reacted with 15 μL of 4% (vol/vol) in each formaldehyde isotope labeling (light CH_2O 37%, medium CD_2O 20%, and heavy $^{13}CD_2O$ 20%). Labeled samples were incubated at 25 °C in a fume hood with shaking for 1 h. Labeled peptides were quenched with 1% (vol/vol) ammonia solution on ice. Samples were pooled and dried using Speed-Vac.

For phosphoproteomics, labeled peptide samples were enriched using the High-Select TiO_2 Phosphopeptide Enrichment Kit. Afterward, they were fractionated into 20 fractions per sample using the High pH Reversed-Phase Peptide Fractionation Kit (Pierce). Fractionated samples were resuspended in appropriate volume with 0.1% formic acid (FA) before LC−MS/MS analysis.

Quantitative Total Proteome Sample Preparation

The U87MG cells were lysed with 8 M urea, 100 mM TEAB, 1× protease inhibitor, and 1× phosphatase inhibitor. Lysates were centrifuged at 13,000g for 5 min at 4 °C. The BCA assay was performed to determine protein concentrations. Protein sample from each condition was adjusted to 100 μg in 8 M urea lysis buffer. Then, the proteins were reduced, alkylated, and digested similarly to the protocol for phosphoproteomics. Tryptic peptides were further cleaned up with reversed-phase C18 SPE columns. Peptide concentrations were determined. Dimethyl labeling was performed as stated in the phosphoproteomics section.

Next, labeled peptide samples were fractionated into 20 fractions per sample using peptide fractionation by a High pH Reversed-Phase Peptide Fractionation Kit (Pierce). Fractionated samples were resuspended with 0.1% formic acid (FA).

LC−MS/MS Analysis

The peptide fractions for phosphoproteomics or total proteomics were analyzed using the quadrupole Orbitrap Q-Exactive Plus mass spectrometer (Thermo Scientific) with reversed-phase EASY nano-LC 1000 using a 25 cm EASY-Spray C18 column, 75 μm internal diameter. The analytical column was equilibrated with Mobile Phase A (0.1% formic acid in LCMS grade water) and Mobile Phase B (0.1% formic acid in acetonitrile). The column was maintained at a constant flow of 300 nL/min. Peptides were injected at 300 ng and eluted by a 90 min gradient (0−5% B in 0 min, 5−20% B in 60 min, 20−40% B in 20 min, 40−98% B in 2 min, and 98−100% B in 8 min). The electrospray voltage 2.0 kV was applied, and the ion transfer tube was set at 275 °C. Orbitrap precursor spectra were recorded from 350−1400 m/z for 90 min at the resolution of 70,000 with AGC target at 3×10^6 ions and maximum IT 250 ms. Top 10 most abundant precursors with 2+ to 4+ charge states were selected and fragmented by normalized collision energy N(CE) 27 to generate MS/MS data. Data-dependent MS/MS spectra were recorded at the resolution of 17,500, AGC target of 5×10^4 ions, and max ion injection time of 100 ms. Signals with unknown charge states were excluded from fragmentation. The dynamic exclusion option was enabled at 30 s.

LC−MS/MS Data Analysis

All raw MS data were processed using MaxQuant version 1.6.2.10. Data were used to search against a human protein database using Andromeda database peptide search engine. For phosphoproteomic analysis, modifications were interpreted as oxidation (M), acetyl (K), carbamidomethyl (C), phospho (STY), and dimethyl labels. For total proteomic analysis, modifications were interpreted as oxidation (M), acetyl (K), carbamidomethyl (C), and dimethyl labels. Searches with trypsin/P specific enzyme. Mass tolerances for precursor and fragment ions were set to 10 ppm and 0.02 Da. The false

https://doi.org/10.1021/acs.jproteome.2c00240
J. Proteome Res. 2022, 21, 2893−2904

discovery rates (FDR) or q-values of the identified peptides were set at less than 1%. All differential analyses were performed using Perseus platform version 1.5.5.3.

Immunofluorescence Analysis

U87MG cells were cultured in an eight-well chamber slide (Lab-Tek). Cells were starved for 24 h and then activated or treated with AZD8055 for another 24 h before the staining. They were fixed with 4% paraformaldehyde in phosphate-buffered saline (PBS) for 10 min. Subsequently, the cells were permeabilized using 0.2% Triton X-100 buffer and blocked with PBS containing 5% bovine serum albumin and 0.1% Tween-20. The antibodies, including anti-BABAM1, anti-γH2AX, and anti-RAP80 (Cell Signaling), were incubated with the cells at 4 °C overnight. Secondary antibodies were then incubated for 1 h. Zenon Rabbit IgG labeling kit (Invitrogen) was used to conjugate the fluorescent dyes to primary antibodies when necessary. Nuclei were stained with 4′,6′-diamidino-2-phenylindole (DAPI). Slides were mounted with a ProLong anti-fade mountant (Invitrogen). Images were captured by an LSM800 with an Airyscan confocal microscope (Zeiss).

Co-immunoprecipitation and Immunoblotting

Candidate proteins from phosphoproteomics data were validated using co-immunoprecipitation (co-IP) and western blotting analysis. For co-IP steps, Crosslink Magnetic IP/Co-IP Kit (Pierce) was used.Cells were lysed using an IP lysis buffer supplemented with protease inhibitor cocktail and phosphatase inhibitor cocktail. The cell lysates were centrifuged and then incubated overnight at 4 °C with the primary antibody against BABAM1 or RAP80 (Cell Signaling), followed by an incubation with Protein G magnetic beads for 1 h. The immunoprecipitated samples were washed twice with the IP lysis buffer. IP-eluted proteins were separated by SDS-polyacrylamide gel electrophoresis (SDS-PAGE) and immunoblotted with primary antibodies [anti-RICTOR (Abcam), anti-BABAM1, anti-γH2AX, anti-RAP80 (Cell Signaling)]. For immunoblotting, cells were washed with PBS, lysed on ice in the buffer containing 1% Triton X-100 and supplemented with the protease inhibitor cocktail and phosphatase inhibitor cocktail. Proteins were separated by SDS-PAGE and detected by immunoblotting with a primary antibody against pAKT (Ser473), AKT, pS6 (Ser235/236), S6, pH2AX (Ser139), H2AX, and GAPDH (Cell Signaling). Western blotting experiments were performed in three biological replicates.

Cell Viability Assay

Cells were seeded into a 96-well plate at the density of 5×10^3 per well with 100 μL complete medium and cultured under different conditions: activated, AZD8055-treated, rapamycin-treated, or overexpressing BABAM1 (WT or S29A) for 24 h in a humidified, 5% CO_2 atmosphere. Cell viability was determined by MTS assays (MTS assay kit; #ab197010; Abcam) detecting the absorbance at 490 nm using a 96-well plate reader. The assays were performed in three biological replicates.

Apoptosis Assay

U87MG cells were cultured in six-well plates until reaching about 50% confluence. Cells were serum-starved for 24 h, and then, the medium was replaced by 10% FBS DMEM medium with or without AZD8055 to induce apoptosis. After 24 h, cells were harvested, washed with PBS, and resuspended. In addition, to compare the number of apoptotic cells under multiple conditions, including cells under normal, rapamycin-treated, AZD8055-treated, *RICTOR* knockdown, and cells overexpressing BABAM1 (wild-type or S29A mutant), cells were prepared 24−48 h prior to the apoptosis assay. After harvesting the cells, about 1×10^5 cells were resuspended in a mixture of 200 μL of assay buffer, 2 μL of Apopxin Green Indicator, 1 μL of 7-AAD, and 1 μL of CytoCalcein 450 (Apoptosis/Necrosis Detection Kit; #ab176749; Abcam) as stated in the manual instruction. After 30−60 min incubation at room temperature, protected from light, cell apoptotic status was measured by flow cytometry and analyzed by IDEAS software. All experiments were performed in three biological replicates.

RICTOR Knockdown by siRNA and CRISPR-Cas9-Mediated *RICTOR* Knockdown Stable Cell Line Generation

U87MG cells were cultured in DMEM low glucose supplemented with 10% (v/v) FBS and 1% antibiotic-antimycotic at 37 °C under 5% CO_2 condition. For *RICTOR* knockdown by siRNA experiment, human *RICTOR* Accell siRNA (Dharmacon) was incubated with the cells for 72 h (siRNA) following the recommended Accell Delivery protocol.

For the generation of a stable *RICTOR* knockdown GBM cell line, four pairs of CRISPR-Cas9 single-guide RNA (sgRNA) against human *RICTOR* gene were constructed in pSpCas9n(BB)-2A-Puro (PX462) V2.0 plasmid (Table S1). An empty vector without the sgRNA sequence was used to create negative control cells. The plasmids were transfected into U87MG cells using Lipofectamine 3000 (Thermo Fisher). The transfected cells were then selected by puromycin (5 μg/mL) for 72 h. The selected population was recovered and maintained in regular media (DMEM with 10% FBS). *RICTOR* gene expression was determined to confirm the gene knockdown compared to wild-type cells before other experiments were performed using the *RICTOR* knockdown U87MG cell line.

RICTOR Overexpression

To investigate and confirm that mTORC2 could induce BABAM1 phosphorylation on S29 residue, the transient overexpression of the *RICTOR* gene was performed in U87MG cells.

Myc-Rictor plasmid was purchased from Addgene (Addgene 11367). The plasmid was transformed into*Escherichia coli*Stbl3 strain in LB broth with ampicillin at 37 °C (100 μg/mL). Purification of plasmid DNA was performed using QIAprep Spin Miniprep Kit (QIAGEN). The plasmid DNA was transfected into U87MG cells using Lipofectamine 3000 (Thermo Fisher) and incubated for 48 h before cells were harvested, and immunoblotting experiments were performed.

Site-Directed Mutagenesis of BABAM1 (S29A Mutation)

GFP-BABAM1(S29A)-P2A-Blast was cloned using Gibson assembly. Briefly, the vector was prepared by digesting the EF1a-LwCas13a-msfGFP-P2A-Blast plasmid (Addgene 91924) using AgeI-HF and BamHI-HF. The EGFP fragment was PCR-amplified by using Q5 High-Fidelity DNA polymerase and GFP-APEX2-NIK3x plasmid (Addgene 129274) as the template. N and C terminal fragments of BABAM1 (S29A) were PCR-amplified using cDNA from U87MG cells as the template. All the fragments and vectors were assembled by NEBuilder HiFi DNA Assembly and transformed into*E. coli*Stbl3 strain. The sequence was confirmed by next-

https://doi.org/10.1021/acs.jproteome.2c00240
J. Proteome Res. 2022, 21, 2893−2904

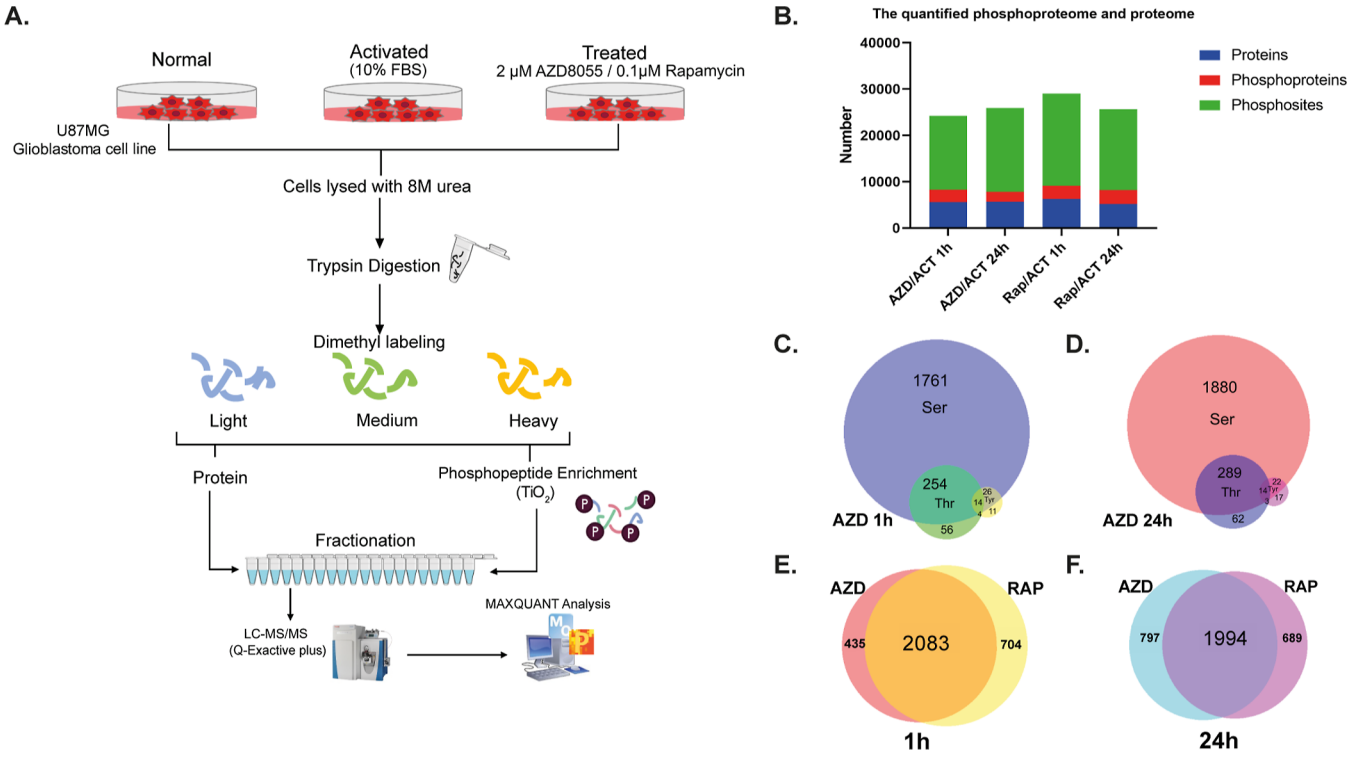

Figure 1. Summary of the phosphoproteomic and proteomic analysis. (A) Workflow for proteome and phosphoproteome analysis. (B) The number of proteins, phosphoproteins, and phosphosites, respectively. (C,D) Venn diagram showing numbers of different phosphopeptides containing S, T, or Y phosphosites in the phosphoproteomic data set from a U87MG cell line with AZD8055 inhibition at two time points, 1 and 24 h, respectively. (E,F) Venn diagram of the overlap of phosphoproteins in the phosphoproteomic data set from the U87MG cell line with 2 μM AZD8055 and 0.1 μM rapamycin treatment at 1 and 24 h, respectively. *RAP/ACT = ratio of rapamycin-treated group to serum-activated group, AZD/ACT = ratio of AZD8055-treated group to serum-activated-group.

generation sequencing-based BT sequencing (U2Bio Thailand). The primers are shown in the Supporting Information (Table S2). To investigate the effect of BABAM1 phosphorylation (Ser29) on cancer cell apoptosis induction, the transient overexpression of *BABAM1*, both wild-type and mutant plasmid, was performed in U87MG cells. The plasmid DNA was transfected into U87MG cells using Lipofectamine 3000 (Thermo Fisher) and incubated for 48 h before related experiments were performed.

RESULTS

Quantitative Phosphoproteome Profiling by mTORC1 and mTORC1/2 Inhibitor

We applied the quantitative phosphoproteomics approaches to characterize the mTOR signaling pathway using dimethyl labeling and phosphopeptide enrichment (TiO_2), followed by fractionation. All mass spectrometry (MS) experiments were performed in five replicates. GBM cells were cultured under three conditions: activation (ACT), mTORC1-inhibiting by rapamycin treatment (RAP), and mTORC1/2-inhibiting by AZD8055 treatment (AZD) at different time points (1 and 24 h). Furthermore, we analyzed 20 phosphopeptide-enriched fractions to achieve high phosphoproteome coverage (Figure 1A and Table S3). We identified over 5,000 total proteins and acquired 15,984 phosphosites in AZD 1 h, 18,076 phosphosites in AZD 24 h, 19,860 phosphosites in RAP 1 h, and 17,431 phosphosites in RAP 24 h (Figure 1B). We displayed the number of individual phosphopeptides containing phosphorylated serine, threonine, and tyrosine residues identified in the U87MG cells treated with AZD8055 or rapamycin for 1 and 24 h in Figures 1C,D and S1, respectively. From the results, we could determine that our drug treatment conditions did not affect the overall global phosphorylation pattern. Also, the number of phosphoproteins identified from the cells treated with AZD8055 and rapamycin for 1 and 24 h is shown (Figure 1E,F).

Functional Analysis of Phosphoproteome Reveals Phosphoprotein Clustering Influenced by mTOR Signaling Inhibition

We examined the phosphorylation profiles, identified the phosphoproteins downregulated by over two-fold in AZD8055-treated compared to activated GBM cells (AZD/ACT) and rapamycin-treated compared to activated cells (RAP/ACT) at 1 and 24 h and further analyzed using gene ontology (GO) annotations from DAVID bioinformatics analysis. Top five enriched annotations in each GO term category: molecular function, cellular component, and biological process of downregulated phosphoprotein over two-fold with significant *p*-values ($p < 0.05$) were illustrated. We showed that the downregulated phosphoproteins in AZD/ACT (1 h) were highly associated with nucleosomal DNA binding, chromosome condensation, and chromatin silencing (Figure 2A). In AZD/ACT (24 h) condition, it was also associated with chromosome condensation, eukaryotic initiation factor 4E binding and regulation of DNA repair (Figure 2B). In contrast, the downregulated phosphoproteins in RAP/ACT (1 h) corresponded to cell−cell adhesion, glycolytic process, and translational elongation (Figure 2C). The RAP/ACT (24 h) group represented stress fiber, DNA recombina-

https://doi.org/10.1021/acs.jproteome.2c00240
J. Proteome Res. 2022, 21, 2893−2904

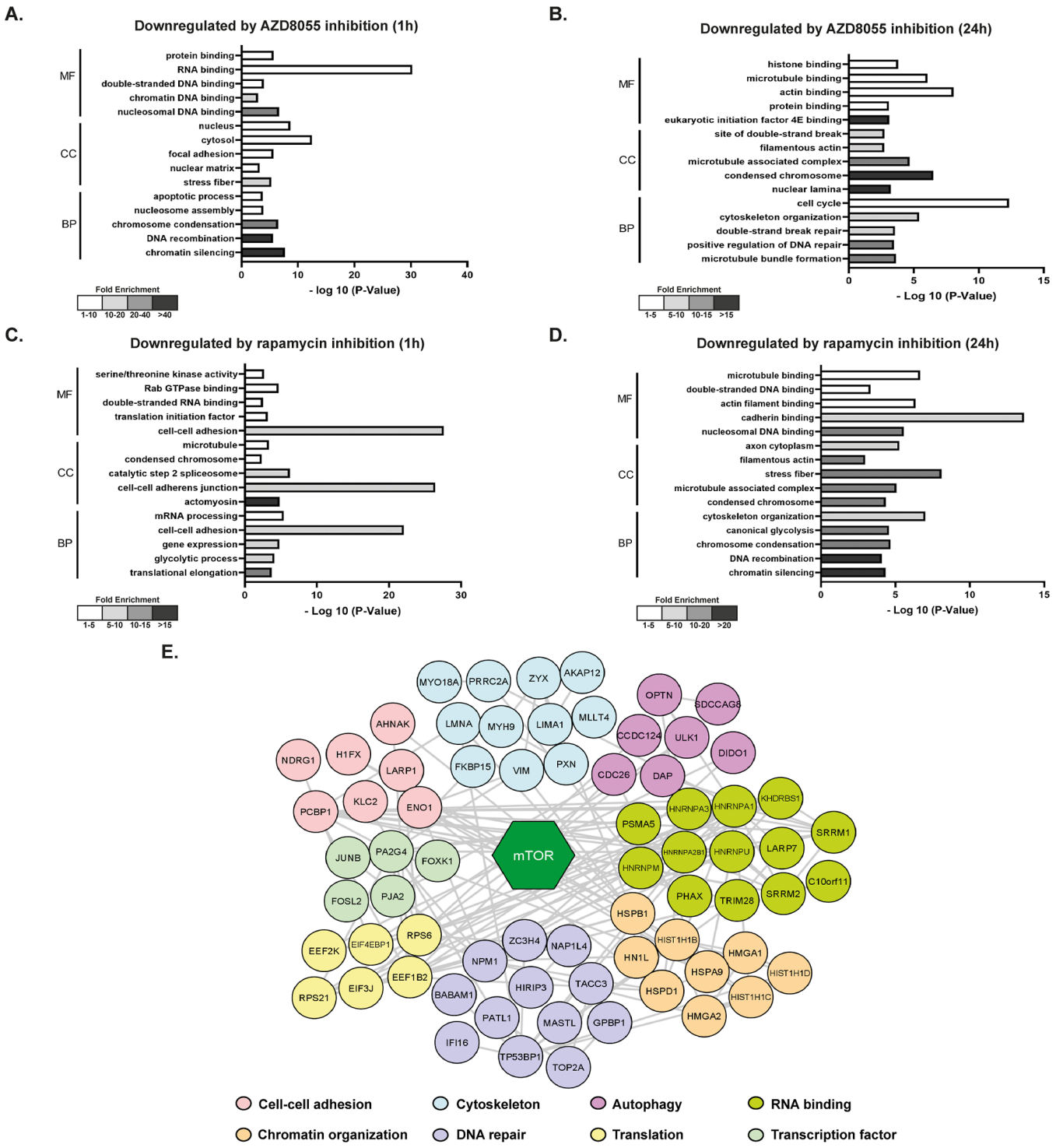

Figure 2. Functional analysis of phosphoproteome affected by AZD8055 and rapamycin treatments. (A,B) All significantly downregulated phosphoproteins in the AZD/ACT group (1 and 24 h). (C,D) All significantly downregulated phosphoproteins in the RAP/ACT group (1 and 24 h), respectively; a ratio of 1 means no change, >1 means upregulated, and <1 means downregulated. GO annotation was done by DAVID bioinformatics resources (https://david.ncifcrf.gov/). Greyscale bar indicates the log2 fold change. (E) Classification of functionally related phosphoproteins and phosphoprotein interactions involved in the mTOR pathway.

tion, and chromatin silencing (Figure 2D). The Cytoscape platform provided and indicated previously known protein−protein interactions. To demonstrate the functions of mTOR signaling in GBM cells, we explored the phosphoproteome data set and focused on the phosphoproteins in the AZD/ACT group, whose signal decreased more than two-fold after 1 h of drug treatment. We detected 70 phosphoproteins involved with the mTOR signaling pathway. The functionally related proteins were classified into eight clusters: cell−cell adhesion, cytoskeleton, autophagy, RNA binding, chromatin organization, DNA repair, transcription factor, and translation (Figure 2E).

https://doi.org/10.1021/acs.jproteome.2c00240
J. Proteome Res. 2022, 21, 2893−2904

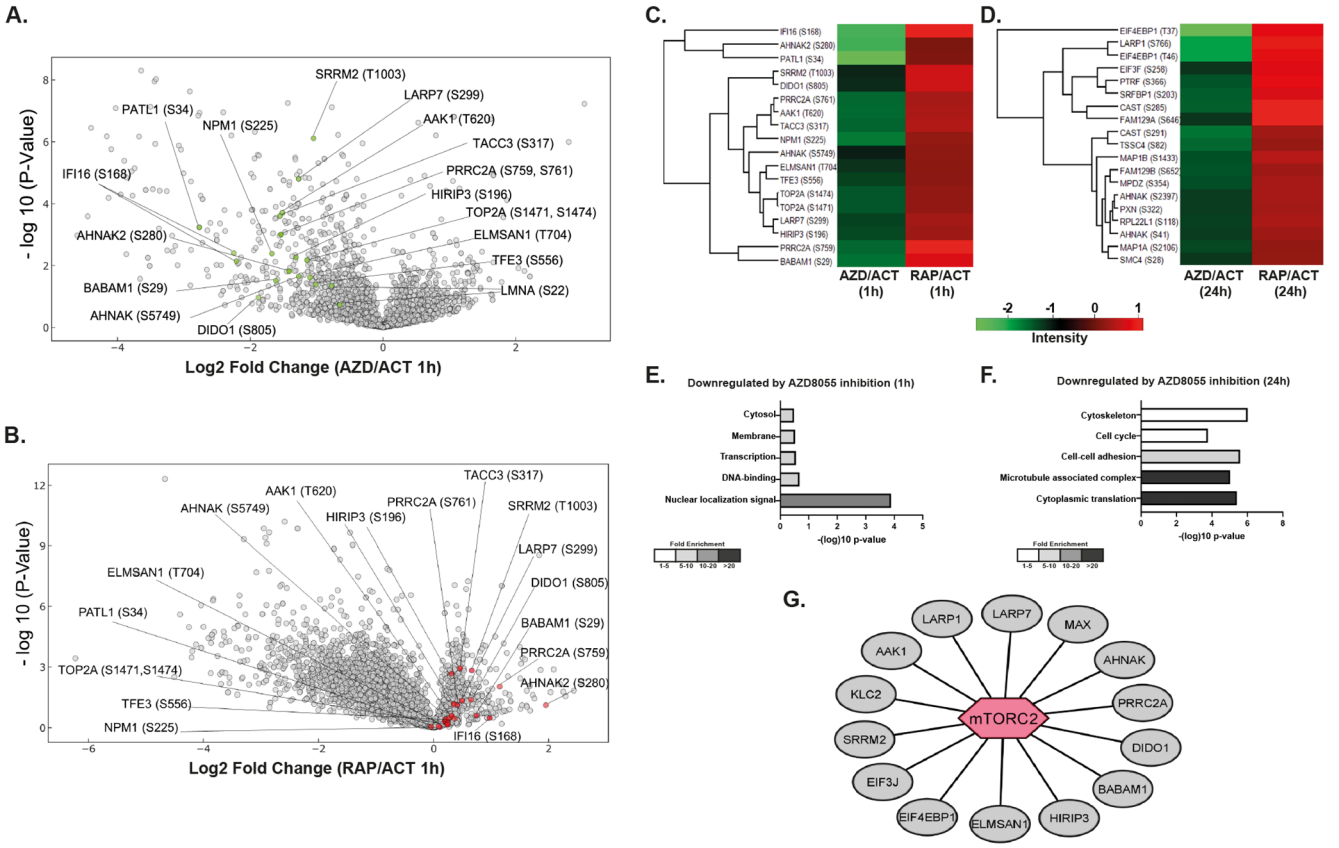

Figure 3. Investigation of mTORC2-mediated phosphorylation events and functional analysis of mTORC2 downstream targets. (A) Volcano plot showing the distributions of phosphosite ratio and *p*-value of the AZD/ACT group (1 h inhibition). (B) Volcano plot showing the distributions of phosphosite ratio and *p*-value of the RAP/ACT group (1 h inhibition). Identical phosphopeptides with opposite fold changes are shown in colors. Proteins in green dots were downregulated in AZD/ACT (1 h), and red dots were upregulated or significantly less downregulated in RAP/ACT (1 h). (C,D) Heatmaps showing the log2 ratio of representative phosphosites with significant data (*p*-value < 0.05). The common phosphopeptides were upregulated in the RAP/ACT group and downregulated in the AZD/ACT group at 1 and 24 h, respectively; a ratio of 1 means no change, >1 means upregulated, and <1 means downregulated. (E,F) Functional annotations of the phosphoproteins with over two-fold difference in the AZD/ACT group compared to RAP/ACT group at 1 and 24 h, respectively. (G) Candidate phosphoproteins involved in the mTORC2 signaling pathway.

Defining the Potential Targets in the mTORC2 Signaling Pathway

For the bioinformatics analysis, we need to determine whether proteins with altered phosphorylation patterns are associated with mTORC2 functions in glioblastoma cells. According to the functional analysis results, the cellular activities significantly affected by AZD8055 but not downregulated by rapamycin treatment were possibly mTORC2-specific processes. Hence, we filtered for the same phosphosites in AZD/ACT and RAP/ACT groups, where phosphorylation events changed significantly ($p < 0.05$). We selected the average log2 ratio values of phosphopeptides in the AZD/ACT group that were less than −1, indicating that the AZD8055 lowered their amounts by more than two-fold. Then, we further determined which identical phosphosites had the average log2 ratio of AZD/ACT lower than the log2 ratio of RAP/ACT over 1, referring to upregulation compared to the AZD8055-treated after rapamycin treatment (Tables S4 and S5). For the 1 h treatment group, we discovered 18 phosphosites that were downregulated in AZD/ACT (green dot) while being upregulated in RAP/ACT (red dot), including AAK1 (Thr620), AHNAK (Ser5749), BABAM1 (Ser29), DIDO1 (Ser805), EIF3J (Ser11), EIF4EBP1 (Thr37), ELMSAN1 (Thr704), HIRIP3 (Ser196), KLC2 (Ser505), LARP1 (Ser766), LARP1 (Ser774), LARP1 (Ser850), LARP7 (Ser299), LARP7 (Ser300), MAX (Ser11), MAX (Ser2), PRRC2A (Ser761), and SRRM2 (Thr1003) (Figure 3A,B). mTORC2 could potentially regulate the phosphorylation of these residues.

The log2 ratio of selected phosphopeptide abundance of RAP/ACT and AZD/ACT, 1 and 24 h treated samples, showed different cluster profiles. The phosphopeptides found to have the highest changed phosphorylation levels in AZD8055-treated cells compared to rapamycin inhibition were depicted. These phosphorylated proteins at specific residues were significantly decreased after the AZD8055 treatment (Figure 3C,D). Excitingly, we found that phosphorylation of BABAM1 on serine 29 was reduced by over four-fold compared to the RAP/ACT group (Table S4 and Figure S2) and almost disappeared after 6 h of AZD8055 treatment. We supposed that BABAM1 (Ser29) might be an important phosphorylation site, and this protein could be a potential mTORC2 downstream effector. Similarly, the phosphorylation of PRRC2A on Ser761, SRRM2 on Thr1003, and ELMSAN1 on Thr704 are poorly known to have biological significance related to the mTORC2 pathway. In addition, we discovered a novel site of KLC2 on Ser505 that has not yet been

https://doi.org/10.1021/acs.jproteome.2c00240
J. Proteome Res. 2022, 21, 2893−2904

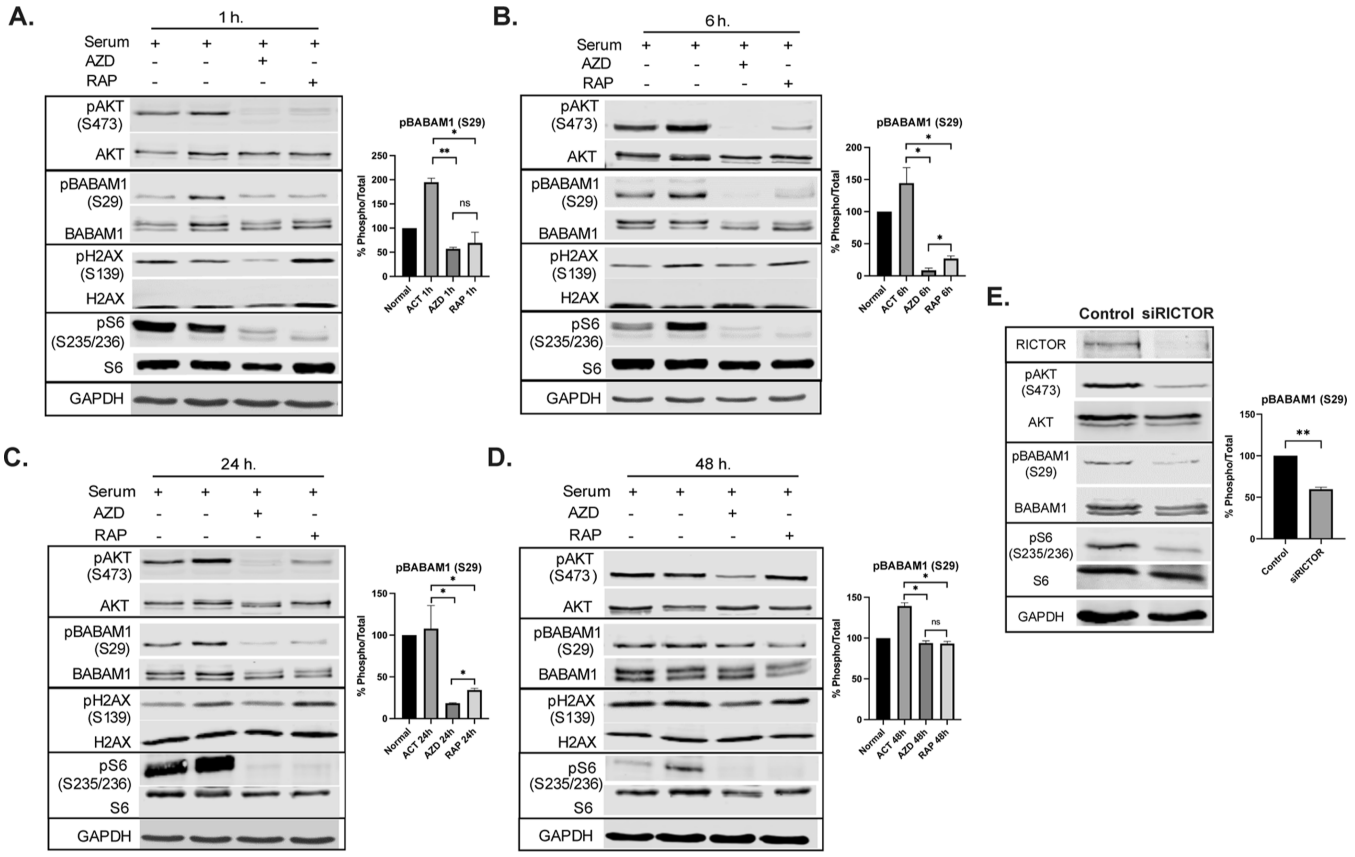

Figure 4. Effects of mTOR inhibitors on BABAM1 activity via mTORC1/mTORC2 signaling. (A–D) U87MG cells were activated with 10% FBS, treated with 2 μM AZD8055 or 0.1 μM rapamycin for 1, 6, 24, and 48 h. (E) U87MG cells were transfected with scrambled siRNA as a negative control group or RICTOR siRNA for 72 h; $n = 3$ biological replicates. Statistical significance was calculated using unpaired two-tailed Student's t-test. All data are mean ± SD: $*p < 0.05$, $**p < 0.01$, ns = not significant.

investigated. Among all potential targets identified from the phosphoproteomic data set, it is important to take into account that all the changes in phosphorylation levels acquired from the analyses must exceed the effects of treatments on the total amount of unmodified proteins. Otherwise, the decrease of phosphorylated peptides observed might only be artifacts from fewer total peptides of each specific protein. To overcome this concern, we have performed the whole cell lysate proteomics using U87MG cells under identical conditions to confirm that the drug treatments did not significantly decrease the total protein levels of any final candidates reported in our study (Figure 3G) when treated with AZD8055 (Figure S3 and Tables S6 and S7). Although a few proteins exhibited significant decreases after 24 h drug treatment, the differences were smaller than the fold changes of their corresponding phosphopeptides compared between ACT and AZD groups. Alternatively, other techniques such as western blotting could be performed as a follow-up experiment to help validate the phosphorylation levels of target proteins after treatments.

In the functional analysis, we analyzed the phosphoproteins that were over two-fold downregulated in AZD/ACT and upregulated in RAP/ACT groups at 1 and 24 h to investigate the strongly affected mTORC2 functions. The most enriched process from the 1 h mTORC2 inhibition group was the nuclear localization signal (Figure 3E), while the cytoskeleton was the most affected GO term when inhibiting mTORC2 for 24 h (Figure 3F). Changes observed in phosphorylation levels of identified phosphoproteins upon AZD8055 treatment could be characterized as players in the mTORC2 signaling. As a result, we discovered several potential novel targets in the mTORC2 signaling pathway in GBM (Figure 3G). In addition to the direct effectors of mTORC2 that were highly downregulated after AZD8055 treatment, our study also provided an informative data set regarding mTORC2 functions related to negative and positive feedback mechanisms, crosstalk cascades, or the cellular responses to pathway inhibition when considering upregulated phosphoproteins (Tables S8 and S9). Further investigations would help elucidate more mechanistic regulations associated with this signaling pathway.

BABAM1 is a Potential mTORC2 Downstream Effector

AZD8055 is a small molecule ATP-competitive inhibitor of mTORC1/2 that directly affects AKT activation by decreasing the phosphorylation at Ser473.[10] We investigated the effects of the AZD8055 treatment on BABAM1 phosphorylation at Ser29, in parallel with the phosphorylation of histone H2AX (Ser139) or γH2AX. Both proteins have been known as markers of DNA damage and genomic instability.[11,12] The western blotting analysis results showed that mTORC2 inhibition significantly reduced pBABAM1 (Ser29) (Figure 4A–D). In contrast, inhibition of mTORC1 alone with rapamycin showed a lower degree of reduction in pBABAM1 (Ser29) and γH2AX levels. Significant differences between pBABAM1 (Ser29) in AZD8055- and rapamycin-treated samples could be detected in the 6 and 24 h groups. Additionally, *RICTOR* knockdown was able to inhibit phosphorylation of BABAM1 at Ser29 and γH2AX (Figure

https://doi.org/10.1021/acs.jproteome.2c00240
J. Proteome Res. 2022, 21, 2893−2904

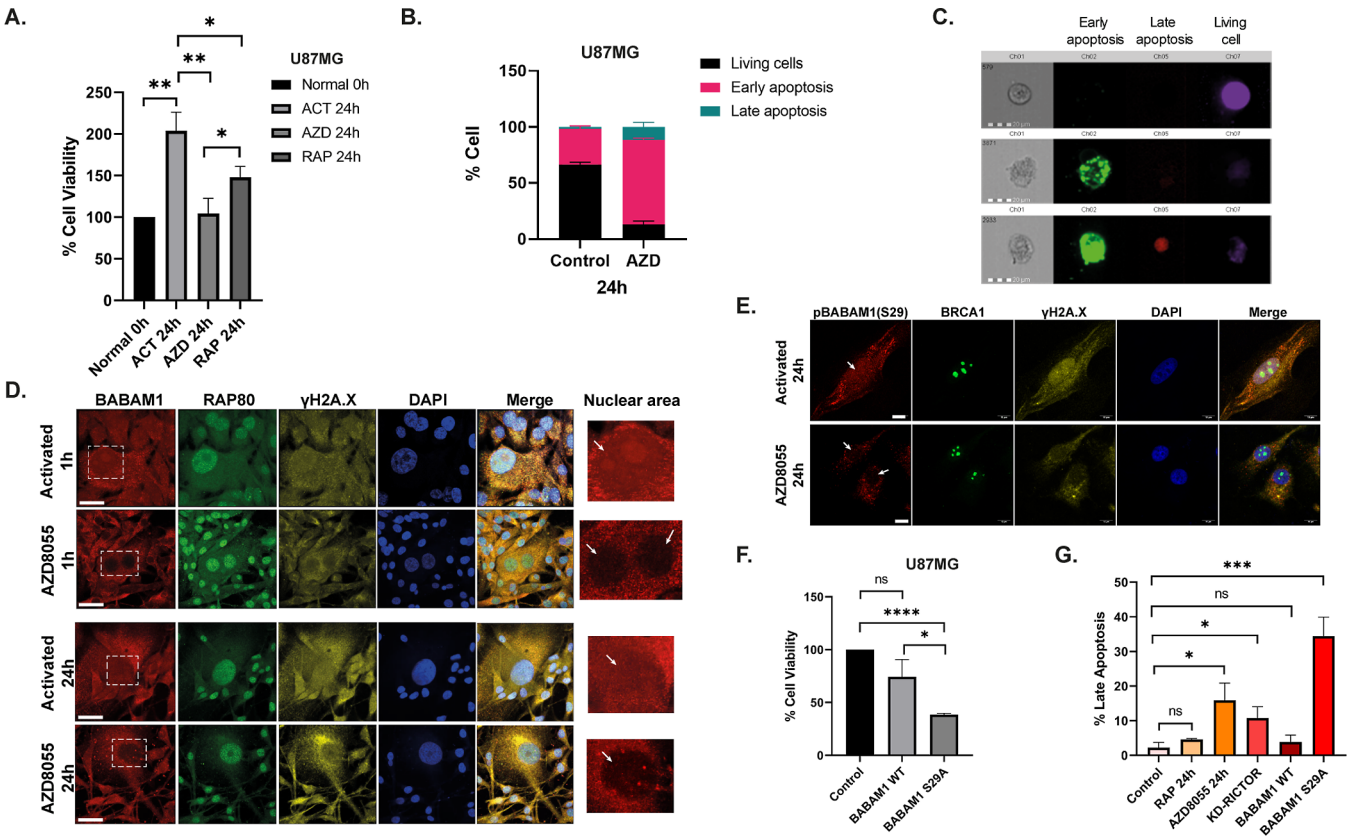

Figure 5. mTORC2 affects the cellular response to DNA damage in glioblastoma. (A) Percent cell viability of U87MG cells under different culturing conditions. (B) The bar graph shows the proportion of cells between living cells and apoptosis states. (C) Single-cell morphology between living cells and cells under apoptotic states analyzed by an imaging flow cytometer, including living cell (violet-stained), early apoptosis (green-stained), and late apoptosis (green- and red-stained) (D) Immunofluorescence staining: U87MG cells were treated with 2 μM AZD8055 for 1 and 24 h and subjected to immunofluorescence staining with anti-BABAM1 (red), anti-RAP80 (green), and anti-γH2AX (yellow) antibodies. Cell nuclei were stained with DAPI (blue). Scale bar, 20 μm. Magnified images of the nuclear area (dashed boxes) are shown. (E) Immunofluorescence staining: U87MG cells were treated with 2 μM AZD8055 for 24 h and stained with anti-pBABAM1(Ser29) (red), anti-BRCA1 (green), and anti-γH2AX (yellow) antibodies. Cell nuclei were stained with DAPI (blue). Scale bar, 10 μm. (F) Cell viability of U87MG-overexpressing BABAM1 (wild-type or S29A) compared to the control group. (G) Percentages of late apoptotic cells in U87MG under different treatment conditions. Statistical significance was calculated using unpaired two-sided Student's *t*-test. All data are mean ± SD: $*p < 0.05$, $**p < 0.01$, $***p < 0.001$, $****p < 0.0001$, ns = not significant.

4E). This part suggested that mTORC2 might play a critical role in regulating DNA damage and repair, similarly to what we defined when performing GO analysis. We also performed transient overexpression of RICTOR and determined that pBABAM1 (Ser29) was significantly increased (Figure S4).

mTORC2 Reveals the Cellular Response to DNA Damage

We performed MTS assays to determine the effects of mTORC1/2 activity on cell survival after AZD8055 and rapamycin exposure. Bar graphs showed the percentage of cell viability when U87MG cells were activated with 10% FBS, treated with 2 μM AZD8055 and 0.1 μM rapamycin after 24 h. Cell proliferation was significantly increased when activated with 10% FBS for 24 h. Both drug treatments substantially prevented cell proliferation. However, AZD8055 delivered more stronger effects on cell viability than rapamycin. The effect of AZD8055 on U87MG proliferation was significant when compared to rapamycin-treated cells (Figure 5A), leading to the hypothesis that mTORC2 inhibition by AZD8055 might induce apoptosis in GBM. We detected apoptosis using the Apoptosis/Necrosis Detection Kit (Abcam) and counted the number of cancer cells under different states by flow cytometry (Figure 5B). Single U87MG cells were observed with a different morphology of cells: living (violet-stained), early apoptotic (green-stained), and late apoptotic (green- and red-stained) cells (Figure 5C).

Interestingly, we detected that U87MG cells showed a larger proportion of early apoptosis and late phase of apoptosis when treated with 2 μM AZD8055 than the control group. The characteristic dot plots indicating the flow cytometric valuation of apoptosis compared to the control are shown in Figure S5. This evidence supported that mTORC2 inhibition impaired DNA repair mechanisms and promoted apoptosis.

Next, we examined the localization of BABAM1. Colocalization of BABAM1, BRCA1-A complex subunit RAP80, and γH2AX, the marker for DNA damage, in serum-activated and AZD8055-treated U87MG cells was observed by immunofluorescence staining. BABAM1 colocalized with γH2AX and RAP80 in the nucleus and cytosol in mTORC2-activating conditions in both 1 and 24 h groups (shown in orange). At the same time, AZD8055-treated cells demonstrated colocalization of BABAM1 and γH2AX, particularly around the perinuclear region and cytosol but not in the nucleus. After 24 h of drug treatment, the aggregation of BABAM1 and γH2AX outside the nucleus was clearly observed (Figure 5D). The results suggested that the colocalization of BABAM1 and

https://doi.org/10.1021/acs.jproteome.2c00240
J. Proteome Res. 2022, 21, 2893−2904

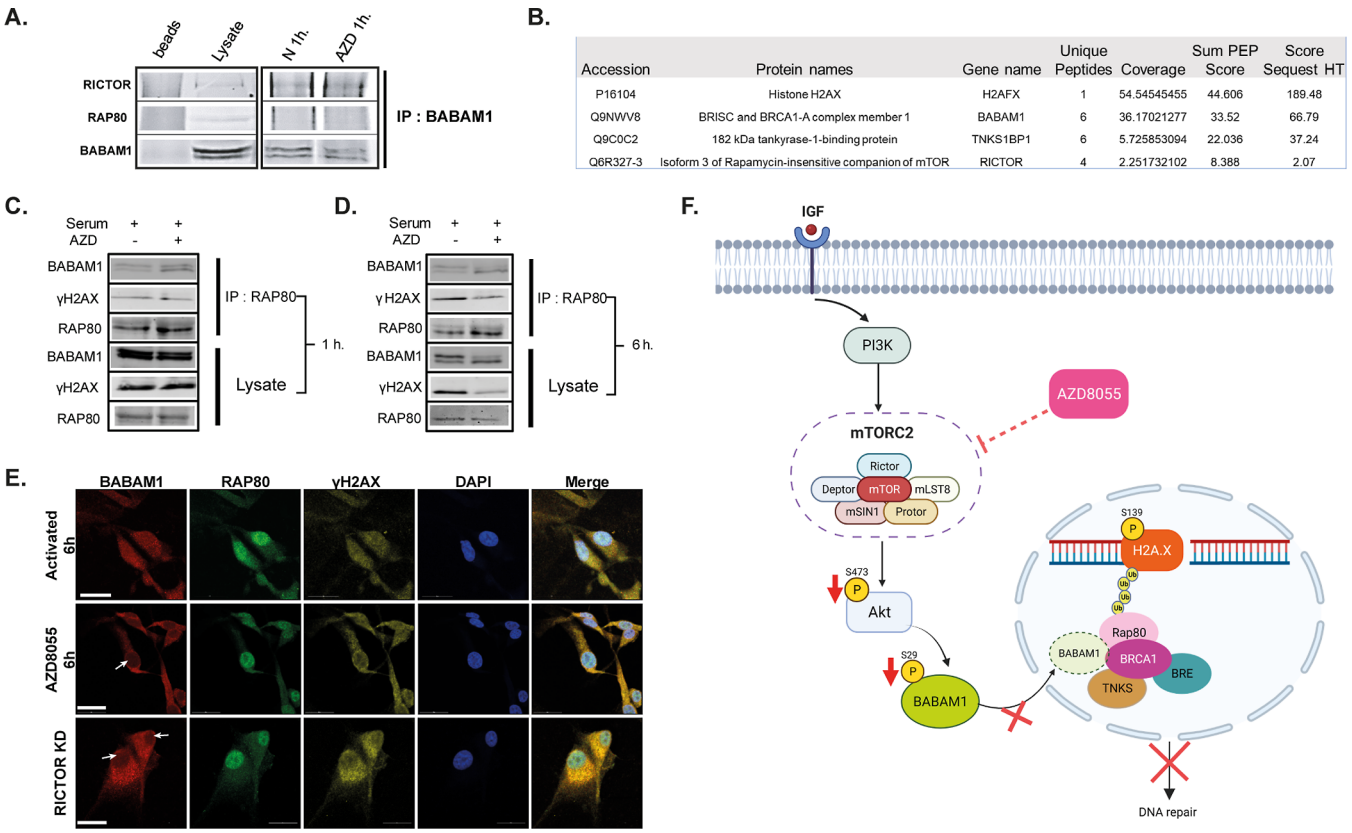

Accession	Protein names	Gene name	Unique Peptides	Coverage	Sum PEP Score	Score Sequest HT
P16104	Histone H2AX	H2AFX	1	54.54545455	44.606	189.48
Q9NWV8	BRISC and BRCA1-A complex member 1	BABAM1	6	36.17021277	33.52	66.79
Q9C0C2	182 kDa tankyrase-1-binding protein	TNKS1BP1	6	5.725853094	22.036	37.24
Q6R327-3	Isoform 3 of Rapamycin-insensitive companion of mTOR	RICTOR	4	2.251732102	8.388	2.07

Figure 6. BABAM1 is a downstream target of mTORC2 signaling pathway in glioblastoma. (A) BABAM1 was immunoprecipitated from U87MG cells under two conditions: activated or treated with 2 μM AZD8055 for 1 h. RICTOR was discovered in the BABAM1 IP sample, confirming the relationship between mTORC2 and BABAM1. (B) The table represents key proteins associated with BABAM1 identified from the co-IP samples from (A). (C,D) RAP80 was immunoprecipitated from U87MG cells treated with 2 μM AZD8055 for 1 and 6 h. (E) Immunofluorescence staining: U87MG cells were activated with serum, treated with 2 μM AZD8055, and knockdown *RICTOR* for 6 h. Stained with anti-BABAM1 (red), anti-RAP80 (green), and anti-γH2AX (yellow) antibodies. Cell nuclei were stained with DAPI (blue). Scale bar, 20 μm. (F) A schematic model of mTORC2-mediated BABAM1 regulation and DNA damage response. The graphic was created by BioRender.com.

γH2AX in the perinuclear region might be associated with mTORC2 inhibition and responsible for the reduction of DNA repair machinery assembly in the nucleus. We further validated the association between phosphorylated BABAM1 (Ser29) and its key interacting partner, BRCA1, under mTORC2-inhibiting conditions by immunofluorescence staining. The colocalization of BRCA1 and pBABAM1 in the nucleus was observed in an activation condition. In contrast, when pBABAM1 (Ser29) was inhibited by AZD8055 treatment, the nuclear localization of BABAM1 protein and the formation of the BRCA1-A complex were strongly affected, while U87MG cells under rapamycin treatment showed similar results as the activated cells (Figures 5E and S6). To determine whether BABAM1 phosphorylation at Ser29 residue promotes DNA repair in GBM cells and the loss of pBABAM1 (Ser29) would lead to cell apoptosis, we transiently overexpressed the BABAM1 S29A mutant in U87MG cells in comparison to wild-type BABAM1 and the control cells (Figure S7). We found that the proliferation of GBM cells was significantly affected in the mutant group when observed at 48 h after plasmid transfection. However, the overexpression of wild-type BABAM1 did not induce cell proliferation in the GBM cells (Figure 5F). Next, we performed apoptosis assays and analyzed for percentages of late apoptotic cells in the samples from various conditions. As expected, GBM cells from mTORC2-inactivating conditions (AZD8055 and *RICTOR* knockdown) showed high late apoptosis rates as well as BABAM1 (S29A)-expressing cells, while cells treated with rapamycin or overexpressing wild-type BABAM1 did not significantly promote apoptosis in GBM (Figures 5G and S8).

mTORC2-Mediated BABAM1 Phosphorylation at Ser29 Promotes DNA Repair

Finally, we performed affinity purification mass spectrometry (AP-MS) to confirm that BABAM1 is regulated by mTORC2 signaling. The western blotting analysis and mass spectrometry analysis of immunoprecipitated BABAM1 in the activated and AZD8055-treated U87MG cells. We found multiple components involved with DNA damage response (DDR) (Table S10), such as tankyrase-1 binding protein (TNKS1BP1) and γH2AX, co-purified with BABAM1. Moreover, we retrieved RICTOR, a major component of mTORC2, indicating that mTORC2 might be physically interacting with BABAM1. However, we could not detect RAP80 in the western blot or MS data. The absence of RAP80 might be because some interacting proteins retrieved were less than a detectable level (Figure 6A,B). Then, we confirmed that the protein−protein interactions among BABAM1, γH2AX, and RAP80 under mTORC2-activating and -inactivating conditions were different by pulling down RAP80. We also included the 6 h AZD8055 treatment condition for this experiment because the global phosphoproteome data set showed that the phosphorylation of BABAM1 at Ser29 was reduced by more than two-fold after 1 h (Table S4) and was more reduced after 6 h with

https://doi.org/10.1021/acs.jproteome.2c00240
J. Proteome Res. 2022, 21, 2893−2904

AZD8055 treatment that it disappeared which correlated with the previous western blot results. We discovered that BABAM1 and γH2AX were less interacting with RAP80 after AZD8055 treatment (Figure 6B,C). In addition, we performed the immunofluorescence staining experiment comparing activated U87MG cells to 6 h AZD8055-treated and stable *RICTOR* knockdown cells. Decreased mTORC2 activity by knocking down *RICTOR* and AZD8055 treatment affected BABAM1 and γH2AX localization to appear mainly outside the nucleus, whereas, in cells containing active mTORC2, BABAM1 colocalized with γH2AX both in the nucleus and cytosol (Figure 6D).

Overall results have concluded that BABAM1 and γH2AX interact with the mTORC2 complex. The inhibition of the complex significantly decreased the phosphorylation of BABAM (Ser29) and the level of γH2AX, disabling DNA repair mechanisms (Figure 6F). This study confirmed that BABAM1 is a regulator in mTORC2 signaling that plays a vital role in repairing DNA damages in GBM.

DISCUSSION

The aberrant mTOR signaling plays an essential role in tumorigenesis and abnormal development. Overactivation of mTOR signaling can lead to several key features such as cell growth, metastasis, invasion, and DNA damage response of different types of cancer cells.[13,14]

While mTORC1 has been thoroughly elucidated, studying the functions of mTORC2 has been a challenging task because very few mTORC2-specific inhibitors have been developed.[15] In recent years, mTORC2 has been shown to play a crucial role in several biological processes of cancer cells, including cell survival, proliferation, cytoskeletal reorganization, metabolic reprogramming, and cellular stress response.[16−18] Hyperactivated mTORC2 is one of the characteristics of GBM.[19] Therefore, the resistance to rapamycin has been a critical concern and likely contributes to the low efficacy of drug treatment in glioblastoma patients.[2]

Recently, phosphorylation events have been widely recognized as a central player in the tumor growth of human glioblastoma.[20] In a phosphoproteomics study, the authors reported no changes in stemness marker gene expression after therapy responsive and recurrence or resistance in the GBM model.[21] Moreover, the phosphoproteomic analysis could help identify targets for drug treatment in GBM patients.[22] Apart from the phosphorylation events in GBM, it is crucial to understand the molecular mechanisms underlying the aberrant signaling to develop potential therapeutic targets.[23]

Here, we performed the phosphoproteomic analysis of U87MG glioblastoma cells treated with the mTORC1/mTORC2 inhibitor, AZD8055, compared with the mTORC1 inhibitor, rapamycin, to define novel mTORC2 targets and functions. Several phosphoproteins involved in mTORC2 signaling were identified. One exciting and significant change was the phosphorylation of BABAM1 at Ser29, which plays an important role in DNA damage response and repair.

BABAM1 is a component of the BRCA1-A complex that directs DNA repair. The BRCA1-A complex, including breast cancer 1 (BRCA1), BRISC and BRCA1-A complex member 2 (BRE), Lys-63-specific deubiquitinase BRCC36, BRCA1-A complex subunit Abraxas 1 (ABRAXAS1), RAP80, and BABAM1, forms at sites of DNA double-strand breaks (DSBs) and contributes to DNA damage repair. BABAM1 functions by stabilizing the BRCA1-A complex.[11] The ubiquitin-binding motifs (UIMs) of RAP80 also help BABAM1 recruit BRCA1-A to the DSBs loci.[24] Then, BRCA1 colocalizes with γH2AX to engage the DNA damage response proteins to repair double-strand breaks.[11] Our study provided evidence that when mTORC2 is inhibited, the colocalization between BRCA1-A complex components, including γH2AX, to promote DNA repair was blocked. Additionally, tankyrase has been reported to associate directly with BABAM1 and form a complex with BABAM1-BRE-BRCC36. Inhibition of tankyrase-BABAM1 or tankyrase-PARP results in abnormal function in DNA repair.[25] In our LC−MS/MS analysis, RAP80, BRCA1, and tankyrase-1 binding protein (TNKS1BP1) were identified.

Previously, Brown et al. reported that purified recombinant AKT1, AKT2, or AKT3 could phosphorylate BABAM1 directly at Ser29. IGF-1 stimulation promoted phosphorylation of BABAM1 and BKM120, MK2206, and Torin1, but not rapamycin could decrease the pBABAM1 (Ser29) level.[26] Remarkably, this correlated with our quantitative phosphoproteomics data. The average log2 fold change of 1 h AZD8055 to activation ratio (AZD/ACT) suggested that pBABAM1 (Ser29) was significantly decreased. The value was over four-fold lower than the rapamycin to activation ratio (RAP/ACT). In addition, the inhibition of mTORC2 depleted AKT phosphorylation at Ser473, while the pBABAM1 level corresponded to pAKT. Consequently, mTORC2 could be the kinase regulating BABAM1 phosphorylation at Ser29 through AKT activation in GBM.

Furthermore, the dual PI3K/mTOR inhibitor NVP-BEZ235 could inhibit the central DDR kinases, DNA-PKcs.[27] AKT directly induces DSB repair by increasing the accumulation of DNA-PK to promote NHEJ[28,29], while mTORC2 regulates F-actin and contributes to the cellular response to minor DNA damage.[30] Moreover, DNA repair pathways often overlap. Thus, affecting one of the pathways should have more impact in a cancer cell with a defective DDR than in a healthy cell.[31] In GBM patients, low BRCA1 protein expression showed a significant correlation with the survival of patients after treatments, indicating that a low level of DNA repair might cause cancer cell vulnerability.[32] Also, BRCA1 has been identified to modulate temozolomide resistance in TP53 wild-type glioblastoma.[33] However, the significance of BABAM1 phosphorylation or its functions in brain cancers have still been unrevealed. Our findings suggest that it could potentially play important roles in GBM cell survival.

CONCLUSIONS

This study provides evidence to support that phosphorylation of BABAM1 at Ser29 is downstream of mTORC2. Without active mTORC2, BABAM1 and H2AX could not initiate DNA damage response and DNA repair in the nuclei, resulting in cell apoptosis. In the future, a specific mTORC2 inhibitor may enable successful therapy for brain cancer patients by disabling DNA repair mechanisms in the cancer cells.

ASSOCIATED CONTENT

Supporting Information

The Supporting Information is available free of charge at https://pubs.acs.org/doi/10.1021/acs.jproteome.2c00240.

List of all common phosphorylation sites (1 h treatment and 24 h treatment) (XLSX)

https://doi.org/10.1021/acs.jproteome.2c00240
J. Proteome Res. 2022, 21, 2893−2904

List of gRNA targeting *RICTOR* gene; list of primers for site-directed mutagenesis of BABAM1 (S29A); summary of the quantified phosphoproteome and proteome in the drug-treated experiments; list of candidate phosphorylation sites (1 h treatment); list of candidate phosphorylation sites (24 h treatment); list of total protein levels of candidate phosphorylation sites (1 h treatment); list of total protein levels of candidate phosphorylation sites (24 h treatment); co-immunoprecipitated proteins identified from BABAM1 IP that are associated with DNA damage response and repair; Venn diagram showing numbers of different phosphopeptides containing S, T, or Y phosphosites in the phosphoproteomic data set; phospho-BABAM1 (Ser29) presented as a log2 fold change; log2 fold change (AZD/ACT) of potential mTORC2 downstream effectors' total proteins and their corresponding phosphorylation sites; Western blotting analysis after RICTOR overexpression in U87MG cells; apoptosis assay using the Apoptosis/Necrosis Detection Kit; immunofluorescence staining of U87MG cells treated with rapamycin for 24 h; Western blotting analysis after BABAM1 overexpression in U87MG cells; relative expression of the *RICTOR* gene; and Western blot membranes performed in the study (PDF)

AUTHOR INFORMATION

Corresponding Author

Naphat Chantaravisoot − *Center of Excellence in Systems Biology, Faculty of Medicine and Department of Biochemistry, Faculty of Medicine, Chulalongkorn University, Bangkok 10330, Thailand;* orcid.org/0000-0003-3946-1798; Phone: +662-256-4482; Email: naphat.c@chula.ac.th

Authors

Nuttiya Kalpongnukul − *Interdisciplinary Program of Biomedical Sciences, Graduate School and Center of Excellence in Systems Biology, Faculty of Medicine, Chulalongkorn University, Bangkok 10330, Thailand*

Rungnapa Bootsri − *Center of Excellence in Systems Biology, Faculty of Medicine and Department of Biochemistry, Faculty of Medicine, Chulalongkorn University, Bangkok 10330, Thailand*

Piriya Wongkongkathep − *Center of Excellence in Systems Biology, Faculty of Medicine and Research Affairs, Faculty of Medicine, Chulalongkorn University, Bangkok 10330, Thailand*

Pornchai Kaewsapsak − *Department of Biochemistry, Faculty of Medicine and Research Unit of Systems Microbiology, Faculty of Medicine, Chulalongkorn University, Bangkok 10330, Thailand*

Chaiyaboot Ariyachet − *Department of Biochemistry, Faculty of Medicine and Center of Excellence in Hepatitis and Liver Cancer, Faculty of Medicine, Chulalongkorn University, Bangkok 10330, Thailand;* orcid.org/0000-0001-8647-7376

Trairak Pisitkun − *Center of Excellence in Systems Biology, Faculty of Medicine and Research Affairs, Faculty of Medicine, Chulalongkorn University, Bangkok 10330, Thailand;* orcid.org/0000-0001-6677-2271

Complete contact information is available at: https://pubs.acs.org/10.1021/acs.jproteome.2c00240

Author Contributions

N.K., N.C., P.W., P.K., C.A., and T.P. participated in the study design. N.K., R.B., and P.K. performed cell-based experiments. N.K. and N.C. carried out imaging experiments, phosphoproteomics, and bioinformatics analysis. N.K. and N.C. wrote the manuscript. N.C., P.W., P.K., C.A., and T.P. provided suggestions on study design and discussion. All authors read, reviewed, edited, and approved the final manuscript.

Notes

The authors declare no competing financial interest.

RAW and MaxQuant-processed proteomics and phosphoproteomics data have been deposited to the PRIDE ProteomeXchange repository (https://www.ebi.ac.uk/pride/login), with the data set accession number PXD033325. Processed data are provided in the supplementary tables in the Supporting Information.

ACKNOWLEDGMENTS

This research was supported by the 100th Anniversary Chulalongkorn University for Doctoral Scholarship, Chulalongkorn University; Ratchadapiseksompotch Funds (grant no. RA62/075), Faculty of Medicine, Chulalongkorn University; the Research Fund for DPST Graduate with First Placement (grant no. 026/2015), the Institute for the Promotion of Teaching Science and Technology (IPST); and the Research Grant for New Scholar (grant no. MRG6180215), Thailand Research Fund (TRF) and the Office of the Higher Education Commission (OHEC). The phosphoproteomic part of this research and innovation activity was funded by National Research Council of Thailand (NRCT). We also would like to express our gratefulness to Tanapati Phakham, Ph.D. and Pijitra Saelao (Center of Excellence in Systems Biology, Faculty of Medicine, Chulalongkorn University) for plasmid DNA preparation.

REFERENCES

(1) Lovely, M. P. Symptom management of brain tumor patients. *Semin. Oncol. Nurs.* **2004**, *20*, 273−283.

(2) Akhavan, D.; Cloughesy, T. F.; Mischel, P. S. J. N.-o. mTOR signaling in glioblastoma: lessons learned from bench to bedside. *Neuro Oncol.* **2010**, *12*, 882−889.

(3) Masui, K.; Cavenee, W. K.; Mischel, P. S. mTORC2 in the center of cancer metabolic reprogramming. *Trends Endocrinol. Metab.* **2014**, *25*, 364−373.

(4) Laplante, M.; Sabatini, D. M. mTOR signaling at a glance. *J. Cell Sci.* **2009**, *122*, 3589−3594.

(5) Mecca, C.; Giambanco, I.; Bruscoli, S.; Bereshchenko, O.; Fioretti, B.; Riccardi, C.; Donato, R.; Arcuri, C. J. F. i. C. N. PP242 counteracts glioblastoma cell proliferation, migration, invasiveness and stemness properties by inhibiting mTORC2/AKT. *Front. Cell. Neurosci.* **2018**, *12*, 99.

(6) Masui, K.; Harachi, M.; Ikegami, S.; Yang, H.; Onizuka, H.; Yong, W. H.; Cloughesy, T. F.; Muragaki, Y.; Kawamata, T.; Arai, N. J. J. o. B. C.; Komori, T.; Cavenee, W. K.; Mischel, P. S.; Shibata, N. mTORC2 links growth factor signaling with epigenetic regulation of iron metabolism in glioblastoma. *J. Biol. Chem.* **2019**, *294*, 19740−19751.

(7) Lamm, N.; Rogers, S.; Cesare, A. J. The mTOR pathway: Implications for DNA replication. *Prog. Biophys. Mol. Biol.* **2019**, *147*, 17−25.

(8) Harsha, H. C.; Pandey, A. Phosphoproteomics in cancer. *Mol. Oncol.* **2010**, *4*, 482−495.

(9) Ramroop, J. R.; Stein, M. N.; Drake, J. M. Impact of Phosphoproteomics in the Era of Precision Medicine for Prostate Cancer. *Front. Oncol.* **2018**, *8*, 28.
(10) Chresta, C. M.; Davies, B. R.; Hickson, I.; Harding, T.; Cosulich, S.; Critchlow, S. E.; Vincent, J. P.; Ellston, R.; Jones, D.; Sini, P.; et al. AZD8055 is a potent, selective, and orally bioavailable ATP-competitive mammalian target of rapamycin kinase inhibitor with in vitro and in vivo antitumor activity. *Cancer Res.* **2010**, *70*, 288−298.
(11) Feng, L.; Huang, J.; Chen, J. J. MERIT40 facilitates BRCA1 localization and DNA damage repair. *Genes Dev.* **2009**, *23*, 719−728.
(12) Mah, L. J.; El-Osta, A.; Karagiannis, T. C. γH2AX: a sensitive molecular marker of DNA damage and repair. *Leukemia* **2010**, *24*, 679−686.
(13) Zou, Z.; Tao, T.; Li, H.; Zhu, X. J. C. mTOR signaling pathway and mTOR inhibitors in cancer: progress and challenges. *Cell Biosci.* **2020**, *10*, 31.
(14) Xie, X.; Hu, H.; Tong, X.; Li, L.; Liu, X.; Chen, M.; Yuan, H.; Xie, X.; Li, Q. The mTOR−S6K pathway links growth signalling to DNA damage response by targeting RNF168. *Nat. Cell Biol.* **2018**, *20*, 320−331.
(15) Werfel, T. A.; Wang, S.; Jackson, M. A.; Kavanaugh, T. E.; Joly, M. M.; Lee, L. H.; Hicks, D. J.; Sanchez, V.; Ericsson, P. G.; Kilchrist, K. V.; et al. Selective mTORC2 Inhibitor Therapeutically Blocks Breast Cancer Cell Growth and Survival. *Cancer Res.* **2018**, *78*, 1845−1858.
(16) Fu, W.; Hall, M. N. J. G. Regulation of mTORC2 signaling. *Genes* **2020**, *11*, 1045.
(17) Chantaravisoot, N.; Wongkongkathep, P.; Loo, J. A.; Mischel, P. S.; Tamanoi, F. J. M. c. Significance of filamin A in mTORC2 function in glioblastoma. *Mol. Cancer* **2015**, *14*, 127.
(18) Oh, W. J.; Jacinto, E. J. C. c. mTOR complex 2 signaling and functions. *Cell Cycle* **2011**, *10*, 2305−2316.
(19) Alvarenga, A. W.; Machado, L. E.; Rodrigues, B. R.; Lupinacci, F. C.; Sanemastu, P.; Matta, E.; Roffé, M.; Torres, L. F.; da Cunha, I. W.; Martins, V. R.; et al. Evaluation of Akt and RICTOR Expression Levels in Astrocytomas of All Grades. *J. Histochem. Cytochem.* **2017**, *65*, 93−103.
(20) Kozuka-Hata, H.; Nasu-Nishimura, Y.; Koyama-Nasu, R.; Ao-Kondo, H.; Tsumoto, K.; Akiyama, T.; Oyama, M. Phosphoproteome of human glioblastoma initiating cells reveals novel signaling regulators encoded by the transcriptome. *PLoS One* **2012**, *7*, No. e43398.
(21) Wei, W.; Shin, Y. S.; Xue, M.; Matsutani, T.; Masui, K.; Yang, H.; Ikegami, S.; Gu, Y.; Herrmann, K.; Johnson, D. J. C. c.; Ding, X.; Hwang, K.; Kim, J.; Zhou, J.; Su, Y.; Li, X.; Bonetti, B.; Chopra, R.; James, C. D.; Cavenee, W. K.; Cloughesy, T. F.; Mischel, P. S.; Heath, J. R.; Gini, B. Single-cell phosphoproteomics resolves adaptive signaling dynamics and informs targeted combination therapy in glioblastoma. *Cancer Cell* **2016**, *29*, 563−573.
(22) van Linde, M. E.; Labots, M.; Brahm, C. G.; Hovinga, K. E.; De Witt Hamer, P. C.; Honeywell, R. J.; de Goeij-de Haas, R.; Henneman, A. A.; Knol, J. C.; Peters, G. J. J. C. C. R. Tumor Drug Concentration and Phosphoproteomic Profiles After Two Weeks of Treatment With Sunitinib in Patients with Newly Diagnosed GlioblastomaGBM: Tumor Sunitinib Concentrations and Phosphoproteomics. *Clin. Cancer Res.* **2022**, *28*, 1595.
(23) Lubanska, D.; Porter, L. J. D. i. R. Revisiting CDK inhibitors for treatment of glioblastoma multiforme. *Drugs R* **2017**, *17*, 255−263.
(24) Kim, H.; Chen, J.; Yu, X. J. S. Ubiquitin-binding protein RAP80 mediates BRCA1-dependent DNA damage response. *Science* **2007**, *316*, 1202−1205.
(25) Okamoto, K.; Ohishi, T.; Kuroiwa, M.; Iemura, S.-i.; Natsume, T.; Seimiya, H. J. O. MERIT40-dependent recruitment of tankyrase to damaged DNA and its implication for cell sensitivity to DNA-damaging anticancer drugs. *Oncotarget* **2018**, *9*, 35844.
(26) Brown, K. K.; Montaser-Kouhsari, L.; Beck, A. H.; Toker, A. J. C. r. MERIT40 is an Akt substrate that promotes resolution of DNA damage induced by chemotherapy. *Cell Rep.* **2015**, *11*, 1358−1366.
(27) Del Alcazar, C. R. G.; Hardebeck, M. C.; Mukherjee, B.; Tomimatsu, N.; Gao, X.; Yan, J.; Xie, X.-J.; Bachoo, R.; Li, L.; Habib, A. A. J. C. c. r. Inhibition of DNA double-strand break repair by the dual PI3K/mTOR inhibitor NVP-BEZ235 as a strategy for radiosensitization of glioblastoma. *Clin. Cancer Res.* **2014**, *20*, 1235−1248.
(28) Toulany, M.; Kasten-Pisula, U.; Brammer, I.; Wang, S.; Chen, J.; Dittmann, K.; Baumann, M.; Dikomey, E.; Rodemann, H. P. J. C. C. R. Blockage of epidermal growth factor receptor-phosphatidylinositol 3-kinase-AKT signaling increases radiosensitivity of K-RAS mutated human tumor cells in vitro by affecting DNA repair. *Clin. Cancer Res.* **2006**, *12*, 4119−4126.
(29) Toulany, M.; Lee, K.-J.; Fattah, K. R.; Lin, Y.-F.; Fehrenbacher, B.; Schaller, M.; Chen, B. P.; Chen, D. J.; Rodemann, H. P. J. M. C. R. Akt promotes post-irradiation survival of human tumor cells through initiation, progression, and termination of DNA-PKcs−dependent DNA double-strand break repair. *Mol. Cancer Res.* **2012**, *10*, 945−957.
(30) Shimada, K.; Filipuzzi, I.; Stahl, M.; Helliwell, S. B.; Studer, C.; Hoepfner, D.; Seeber, A.; Loewith, R.; Movva, N. R.; Gasser, S. M. J. M. c. TORC2 signaling pathway guarantees genome stability in the face of DNA strand breaks. *Mol. Cell* **2013**, *51*, 829−839.
(31) O'Connor, M. J. Targeting the DNA damage response in cancer. *Mol. Cell* **2015**, *60*, 547−560.
(32) Vassilakopoulou, M.; Won, M.; Curran, W. J.; Souhami, L.; Prados, M. D.; Langer, C. J.; Rimm, D. L.; Hanna, J. A.; Neumeister, V. M.; Melian, E.; et al. BRCA1 Protein Expression Predicts Survival in Glioblastoma Patients from an NRG Oncology RTOG Cohort. *Oncology* **2021**, *99*, 580−588.
(33) Ding, J.; Wu, S.; Zhang, C.; Garyali, A.; Martinez-Ledesma, E.; Gao, F.; Pokkulandra, A.; Li, X.; Bristow, C.; Carugo, A.; et al. BRCA1 identified as a modulator of temozolomide resistance in P53 wild-type GBM using a high-throughput shRNA-based synthetic lethality screening. *Am. J. Cancer Res.* **2019**, *9*, 2428−2441.

https://doi.org/10.1021/acs.jproteome.2c00240
J. Proteome Res. 2022, 21, 2893−2904